Lab on a Chip

Cite this: *Lab Chip*, 2012, **12**, 1210

www.rsc.org/loc

FOCUS

Acoustofluidics 8: Applications of acoustophoresis in continuous flow microsystems

Andreas Lenshof,*[a] Cecilia Magnusson[b] and Thomas Laurell*[ac]

DOI: 10.1039/c2lc21256k

This acoustofluidics tutorial focuses on continuous flow-based half wavelength resonator systems operated in the transversal mode, where the direction of the primary acoustic force acts in plane with the microchip. The transversal actuation mode facilitates integration with up- and downstream microchannel networks as well as visual control of the acoustic focusing experiment. Applications of particle enrichment in an acoustic half wavelength resonator are discussed as well as clarification of the carrier fluid from undesired particles. Binary separation of particle/vesicle/cell mixtures into two subpopulations is outlined based on the different polarities of the acoustic contrast factor. Furthermore, continuous flow separation of different particle/cell types is described where both Free Flow Acoustophoresis (FFA) and binary acoustophoresis are utilized. By capitalizing on the laminar flow regime, acoustophoresis has proven especially successful in performing bead/cell translations between different buffer systems. Likewise, the ability to controllably translate particulate matter across streamlines has opened a route to valving of cells/particles without any moving parts, where event triggered cell sorting is becoming an increasing area of activity. Recent developments now also enable measurements of fundamental cell properties such as density and compressibility by means of acoustophoresis. General aspects on working with live cells in acoustophoresis systems are discussed as well as available means to quantify the outcome of cell and particle separation experiments performed by acoustophoresis.

[a]*Dept. Measurement Technology and Industrial Electrical Engineering, Div. Nanobiotechnology Lund University, Sweden. E-mail: andreas.lenshof@elmat.lth.se; thomas.laurell@elmat.lth.se*
[b]*Dept. Laboratory Medicine, Lund University, Skåne University Hospital, Malmö, Sweden*
[c]*Dept. Biomedical Engineering, Dongguk University, Seoul, South Korea*

Introduction

Ultrasonic standing wave based particle manipulation has been investigated in macroscale chamber models in the last five decades and more recently it has entered the microfluidic arena, offering the integration of new cell and particle manipulation modalities in lab-on-a-chip and micrototal analysis systems.[1] Recent advances have shown that ultrasonic standing wave systems in microfluidic channels, *i.e.* acoustofluidics, well match known methods of manipulating cells and particles such as dielectrophoresis, magnetophoresis and hydrodynamical systems.[2] A comparison of the different techniques is presented in Table 1.

The physical properties of particles/cells that affect the magnitude of the primary axial radiation force, F_{ax}, the major force component in acoustic standing wave manipulation, are density, ρ, speed of sound, c, and the radius, R. These properties, the corresponding data for the suspending medium and the parameters of the sound field compose the equation, F_{ax}. Eqn (1) is a special case of the primary acoustic radiation force as obtained in a one-dimensional plane acoustic standing wave. In the more general case of an arbitrary acoustic field, the primary acoustic radiation force is given by eqn (3). The underlying theory that yields these equations is treated

Foreword

The eighth paper of 23 in the *Lab on a chip* tutorial series of Acoustofluidics deals with applications of acoustophoresis in continuous flow microsystems. Basic unit operations such as concentration, separation and fractionation, as well as more complex fluidic procedures such as valve-less switching and acoustic FACS operations, are presented. Many of the examples involve beads but there are also examples of cell based applications. Some advice of how to handle cells for improved outcome, as well as methods for quantifying separation performance are also presented.
Andreas Lenshof – coordinator of the Acoustofluidics series

thoroughly in the Acoustofluidics tutorial 7 of this series.[10] The sign of the primary radiation force is defined by the material properties of the particle/cell relative to the suspending medium and is summarized by the acoustic contrast factor (Φ), eqn (2). The contrast factor hence reveals whether a particle will move toward the pressure node or the antinode in the acoustic standing wave field. A positive contrast factor results in movement toward the pressure node while a negative contrast factor results in a movement to the antinode.

$$F_{ax} = 4\pi a^3 E_{ac} k \sin(2kz)\Phi \quad (1)$$

where F_{ax} is the acoustic radiation force, E_{ac} is the acoustic energy density, a is the particle radius and z is the distance from pressure anti-node in the wave propagation axis.

$$\Phi = \frac{\rho_p + \frac{2}{3}(\rho_p - \rho_0)}{2\rho_p + \rho_0} - \frac{1}{3}\frac{\rho_0 c_0^2}{\rho_p c_p^2} \quad (2)$$

where ρ_p and ρ_0 are density of particle and fluid, respectively, c_p and c_0 are speed of sound in particle material and fluid, respectively, k is the wavenumber ($2\pi f/c_0$) and Φ is the acoustic contrast factor.

$$F^{rad} = -\left(\frac{4\pi a^3}{3}\right)\nabla\left(f_1\frac{\langle p_1^2\rangle}{2\rho_0 c_0^2} - f_2\frac{3}{4}\rho_0\langle v_1^2\rangle\right),$$
$$f_1 = 1 - \frac{K_p}{K_0}, \qquad f_2 = 2\frac{(\rho_p - \rho_0)}{(2\rho_p + \rho_0)} \quad (3)$$

$$v_p(z) = \frac{2\Phi k a^2 E_{ac}}{3\eta}\sin(2kz) \quad (4)$$

$$F_z^{drag} = -6\pi\eta a v_p \quad (5)$$

where f is the frequency, K_0 is the compressibility of fluid, K_p is the compressibility of particle, p_1 is the pressure field, v_1 is the velocity field, v_p is the particle velocity and η is the dynamic viscosity of the fluid.

The literature is rich in reports on continuous flow microfluidic acoustic manipulation devices such as layered resonators,[11,12] transversal resonators[13,14] and SAW (surface acoustic wave) devices.[15,16] Although they differ in design they often utilize the features of half wavelength resonators with a pressure node located in the centre of the flow channel while antinodes are located at the channel walls. Also, a wealth of reports describe multi-wavelength resonators for particle and cell manipulation and

Andreas Lenshof

Andreas Lenshof is currently employed as a postdoctoral fellow at the Department of Measurement Technology and Industrial Electrical Engineering at Lund University. He received his PhD in Electrical Measurements at Lund University in 2009. He has been working with acoustic microfluidic systems for the last 10 years in both academia and industry. His research is currently focused on acoustic particle and cell manipulation in biomedical applications.

Cecilia Magnusson

Cecilia Magnusson received her PhD in Cell Pathology at Lund University in 2008. She is currently a postdoc at the Department of Laboratory Medicine at Lund University. Her research is focused on using acoustic wave technology to isolate circulating tumor cells from blood.

Thomas Laurell

Professor Thomas Laurell holds a position as Professor in Medical and Chemical Microsensors and has since 1995 built his research activities around microtechnologies in biomedicine (http://www.elmat.lth.se/forskning/nanobiotechnology_and_labonachip). Laurell recently started a new applied nanoproteomics laboratory at the Biomedical Centre in Lund, integrating microfluidics and nanobiotechnology developments with medical research. This research is focused on new microchip technologies in the area of biomedicine, biochemistry, nanobiotechnology with a focus on disease biomarkers, diagnostic microsystems and miniaturised sample processing. Laurell also leads the clinically oriented research environment CellCARE (www.cellcare.lth.se), which targets chip based cell separation utilising ultrasonic standing wave technology (acoustophoresis) as the fundamental mode of separation.

Table 1 Comparison of different principles for microfluidic continuous flow cell/particle manipulation

Principle	Parameters	Flow rates	Concentration	References
Magnetophoresis	Magn. susceptibility, size	83 μL min^{-1}	200 × 10^6 particles per mL	3
Dielectrophoresis	Size, dielectric constant, conductivity	500 μL min^{-1}	6 × 10^7 particles per mL	4
Optical	Size, optical polarizability	20–35 μL s^{-1}	90 000 particles per h	5
Pinched flow	Size	500 μL h^{-1}	500 μL^{-1}	6
Deterministic lateral displacement	Size, shape, compressibility	400 μL s^{-1}	0.005–0.015% (volume fraction)	7
		1 μL s^{-1}	Undiluted blood (40%)	8
Acoustophoresis	Size, density, compressibility	1 L h^{-1}	Undiluted blood (40%)	9

processing in larger flow cells and batch systems as well as systems designed for acoustic trapping and positioning of cells. These systems are, however, not covered in this tutorial and the reader is referred to the Acoustofluidics tutorial 22 for an extensive description of multi-wavelength systems. Acoustofluidics 9 will extend on the theory and application of layered resonators, and systems for acoustic trapping will be outlined in Acoustofluidics tutorials no. 19 and 20.

This tutorial focuses on the applications of continuous flow based half wavelength transversal microfluidic resonators, giving an overview of the most recent developments in cell and particle manipulation. Aspects on cell handling in acoustofluidic systems with regards to cell survival and successful experimental outcome are discussed. The most common techniques to quantify the outcome of cell and particle separations are also outlined.

Applications of acoustophoresis

Continuous flow concentration of cells and particles

In continuous flow mode, the most straightforward acoustophoresis unit operation is to concentrate particles in suspension. This is generally done by focusing particles into a node and thereby depletes the surrounding medium of particles. The flow is subsequently split into a fraction containing the concentrated particles while the particle free medium leaves the system in the other fraction.

One of the early microfluidic continuous cell concentrators was described by Yasuda *et al.*, which used a quartz chamber of a half wavelength width. In this case, red blood cells were concentrated into a single band in the flow cell.[17] Using this setup Yasuda *et al.* examined the release of intracellular components from ultrasonically focused red blood cells and found no damage to the cells. However, the system did not have any solution that separated the concentrated fraction from the medium fluid. This was solved in a follow-up work by the same group, introducing a capillary into the chamber in which the concentrated cell fraction was removed.[18]

Cylindrical capillaries have been used as intrinsic acoustic resonators to concentrate particles in continuous flow mode as described by Goddard and Kaduchak,[19] where a transducer was glued directly to the capillary and the glass walls of the capillary both served as a transmission layer and a reflector, Fig. 1. The acoustic capillary focusing was also proposed as an alternative to hydrodynamic focusing in FACS (fluorescence activated cell sorting) applications where the use of acoustic standing waves could replace the sheath flow responsible for focusing the cells or particles into a single stream.[20] This application has recently also been implemented in a commercial FACS instrumentation, Attune™, marketed by Life Technologies.

Silicon is a material that performs well as the bulk material for microfluidic acoustic resonators with a low acoustic attenuation and high difference in acoustic impedance relative aqueous media. Also, very precise structures can be fabricated, adopting well established manufacturing processes used in the semiconductor and MEMS industries.[21] As it is desirable to observe events inside the channel during acoustophoresis, a glass lid is preferable to use to seal the flow channel. The simple means of anodic bonding of glass to silicon enables hermetic sealing of silicon glass channel structures without the need for an adhesive interface and hence very reproducible bonding of structures can be obtained. A more thorough discussion on the construction of acoustofluidic microstructures is given in the Acoustofluidics tutorial 5 of this series.[21] These facts spurred the development of acoustofluidic microsystems in the early years of this millennium.

Harris *et al.* realized a silicon concentrator chip with one inlet and two outlets where concentrated sample exited through one outlet and clarified medium exited through the other.[11,22] It was constructed as a layered resonator where the particles were concentrated in a nodal plane parallel to the flow. Nilsson *et al.* also presented the first transversal mode operated acoustophoretic silicon device having two outlets for extraction of clarified medium along the sides of the acoustophoresis channel and one central outlet that collected the focused particles.[13] In the transversal mode the standing wave is created perpendicular to the flow in plane with the chip, which is advantageous as the performance of the concentrator could easily be inspected and tuned visually.

An all glass structure provides an even better visibility as there is the possibility to use an inverted microscope. Although the channel cross-section is semi-circular in glass resonators, there have been studies which show that the acoustophoretic performance is equal to the performance of a silicon chip of the corresponding rectangular cross-section, Fig. 2.[23] Wiklund *et al.*[24] used an inverted microscope with a microchannel fabricated in silicon etched through the wafer. The channel was sealed with glass covers on both sides, creating a transparent channel structure.

The corresponding approach has been demonstrated by Shi *et al.* in surface acoustic wave (SAW) actuated microsystems who used two opposing

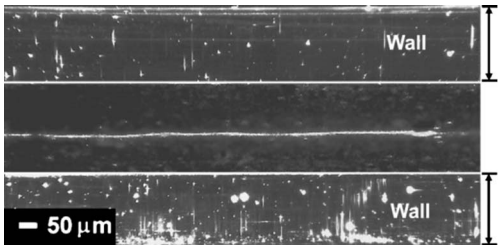

Fig. 1 Photo of cells focused in a glass capillary. Reprinted with permission from Goddard and Kaduchak.[19] Copyright 2005, Acoustic Society of America.

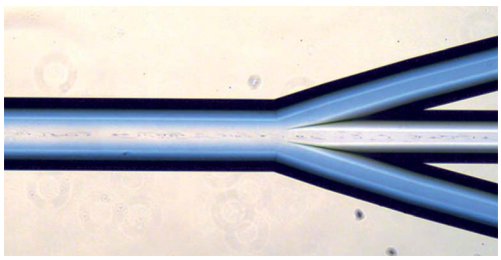

Fig. 2 Glass beads entering along the sidewalls of an acoustophoresis channel in a blue buffer. The acoustophoresis subsequently translates the beads into a stream of uncoloured buffer in the channel centre (continuous flow bead washing). Washed beads exit *via* the central outlet.

interdigitated transducers (IDTs) to generate surface acoustic waves on a piezo-substrate.[15] A PDMS structure was docked between the transducers and the two IDTs produced a standing wave in the liquid channel defined by the PDMS, in which particles were focused in the centre pressure node.

Acoustophoretic filtration/removal of suspended particles

Contrary to concentration, acoustic focusing can be used to remove the solid components, receiving a cell or particle free solution. The same configuration as in the concentration application can be used with a flow splitter after a half wavelength acoustic focusing step.[25,26] However, this basic configuration is only applicable at modest particle concentrations if reasonable particle clearance is to be obtained. What usually fails at high concentrations is the overloading of particles in the central pressure node and consequently loss of beads into the clarified medium fraction. To overcome this problem Lenshof *et al.* reported a device where cells were sequentially removed from the dense stream of cells in the central region of the channel. This enabled the development of a plasmapheresis chip that was capable of handling undiluted whole blood, providing clarified blood plasma.[27] The focused blood cells were removed through exit holes located in the centre bottom of the channel where the density of cells was high. Sequential exit holes lowered the cell concentration gradually and at the end of the separation channel the final fraction of the remaining cells was removed through a flow splitter and blood plasma of low cell counts was obtained that fulfilled the requirements for clinical diagnostics.

Acoustic particle separation

Particle and cell separation using acoustic standing wave technology has been widely researched, where enhanced cell sedimentation is maybe the most common application[28] and currently also is in industrial use *e.g.* in fermentation processes.[29] Sedimentation is accomplished by aggregating particles and cells into the pressure nodal planes of a standing wave. If the nodal planes are aligned with the direction of gravity, the aggregates can be allowed to settle to the bottom of the fluid container. The precondition for this is that the acoustic force resulting from the lateral (parallel to gravity) pressure gradient does not override gravity.

Sedimentation assays have not been widely adopted in the microfluidic domain, whereas aggregation of cells and particles is more commonly employed in the macroscale. Acoustic standing wave aggregation in microfluidic components is typically used in half wavelength resonators where the primary acoustic radiation force levitates the cells/particles into the nodal plane and subsequently the lateral gradient of the primary radiation force drives the cells into a dense cluster in the nodal plane, Fig. 3.

Wiklund *et al.* demonstrated that aggregation of antibody activated microbeads could be used to enhance sensitivity in bead based immunoassays performed in microtiter well plates.[30] Applications using aggregation have to a majority been employed in systems where clusters of cells or particles are trapped and retained over an extended period of time. Some examples of this can be found in the work by Coakley *et al.*,[31] Lilliehorn *et al.*,[32] Vanherberghen *et al.*[33] and Hammarström *et al.*[34] In contrast to acoustic aggregation and trapping, continuous flow based approaches in microfluidic systems can utilize two different modes of flow-based separation, *i.e.* free flow acoustophoresis or binary acoustophoresis.

Size separation by free flow acoustophoresis. In free flow acoustophoresis (FFA) the net acoustic force drives cells or particles (orthogonal to the direction of flow) towards a pressure node at the same time as they travel with the flow.

Basic concepts of performing size based particle separation were landmarked by the early work of Giddings[35] where an external force field is allowed to act on a particle suspension orthogonal to the direction of flow and particles that experience a higher force are translated faster across the laminar flow streams, Fig. 4.

An early implementation of a size separating acoustic standing wave device, based on a half wavelength resonator, was reported by Johnson and Feke in 1995.[36] The system comprised a dual inlet flow with a sample suspension laminated to a main buffer flow that streamed into the acoustic separation area holding a pressure node in the centre of the channel. Larger particles traversed the channel towards the pressure node at a speed proportional to the square of the radius (eqn (4)) and by supplying the device with a split flow outlet in line with the original

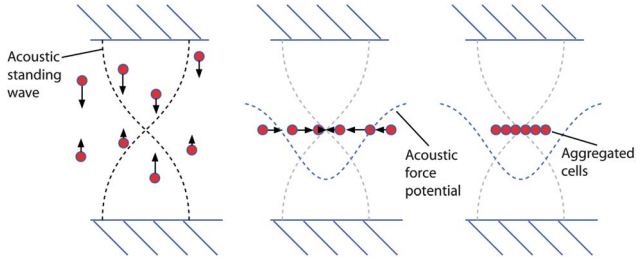

Fig. 3 Schematic of particle aggregation sequence in a half wavelength resonator.

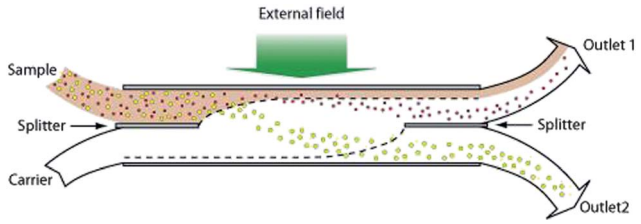

Fig. 4 The principle of the split flow thin (SPLITT) fractionation. A particle mixture enters *via* the sample inlet and as it enters the fractionation chamber the particles are affected by the external force field. The yellow particles experience a larger force than the smaller red particles. The force and the flows are tuned such that the particles that are most affected by the force field travel past the flow splitter and are separated from the smaller red particles.

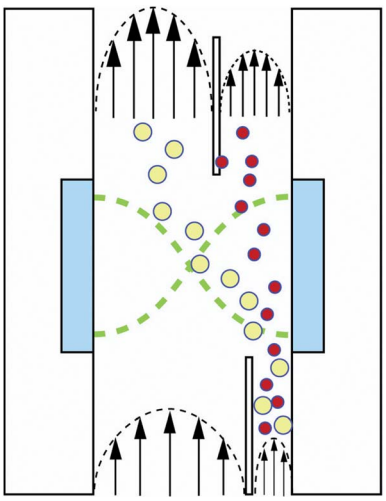

Fig. 5 Schematic of the half wavelength based resonator for particle size separation as reported by Johnson and Feke.[36] The yellow particles experience a larger force than the smaller red ones, and are thus moving faster to the central pressure node. By tuning the flow rate *versus* the acoustic force, a separation is obtained. The piezo actuators are indicated in blue.

SPLITT design, a portion of larger particles (yellow) can be collected from one outlet whereas a fraction with smaller particles (red) is collected from the other outlet, Fig. 5. Later the same group demonstrated the separation of hybridoma cells and *Lactobacillus rhamnosus* cells in a similar setup. Although not being a microfluidic system, as the flow channel was 3.5 mm wide and hence the piezo ceramic actuator was operated at 210 kHz, a proof of concept of FFA based cell separation was given.[37]

Translating this concept into a planar structure, as a microfluidic component actuated in a transversal mode, greatly facilitates integration of in-line particle separation with downstream microfluidic unit operations. Multiple particle or cell fractions can be obtained at the end of the flow channel if the laminar flow is divided into multiple outlets, collecting fractions of particles that have traversed the channel at different speeds in relation to the acoustic force exerted on them. Thereby a fractionation in each outlet is accomplished which corresponds to the net acoustic fingerprint of the population that exits a given outlet. A major factor that determines the acoustic fingerprint is the size of the particle as the primary axial radiation force (eqn (1)) scales with the volume of the particle/cell. The speed of particle movement (eqn (4)), when the F_{ax} is balanced to the Stokes drag on the particle (eqn (5)), is proportional to the square of the radius of the particle and hence size based separation has also been the most commonly used mode of action in realizing a free flow acoustic separator. Fig. 6 schematically outlines the principle of free flow acoustophoresis in multiplex mode separation.

The separation in free flow acoustophoresis mode is controlled by the magnitude of the employed force field and the flow rate, *i.e.* the retention time in the acoustically activated zone. The spatial dimension of a band of given particle size at the channel outlet is defined by two factors, *i.e.* (1) the width of the particle fraction when it enters the separation zone in relation to the channel width and (2) the distance that the particle band traverses the channel before reaching the outlet. The second factor reflects the dispersion of the particle band as a function of the parabolic flow profile from top to bottom of the flow channel (out of plane in Fig. 4) which means that particles display significantly different retention times in the acoustic field and hence have a lateral position in the channel which is dependent on the original location in the flow profile. It should also be pointed out that further dispersion may be observed for suspensions with particle sizes of just a few microns and below. In this case, effects of acoustic streaming start to play a role as the primary acoustic radiation force diminishes rapidly with size and acoustic streaming effects hence become an influential factor to account for. An in-depth discussion on acoustic streaming is treated in Acoustofluidics 13–16 of this tutorial series.

Microchip integrated FFA in a half wavelength transversal resonator was demonstrated by Petersson *et al.* performing continuous flow based separation of polystyrene particle mixtures (2, 5, 7 and 10 micrometre polystyrene beads). Efforts to separate blood erythrocytes, leukocytes and platelets were also reported.[38] FFA has also been reported in microfluidic systems that utilize surface acoustic wave base excitation, where two opposing transducers on a base plate are phase matched to generate a standing wave in the centre of a PDMS channel clamped on top of the base plate. Analogous to Fig. 5 separation of the beads in a sample with 0.9 and 4.2 micrometre polystyrene beads was demonstrated.[16]

Adams *et al.* demonstrated that increased dimensionality in the separation can be accomplished if a combination of magnetic beads and non-magnetic beads is used and both acoustic and

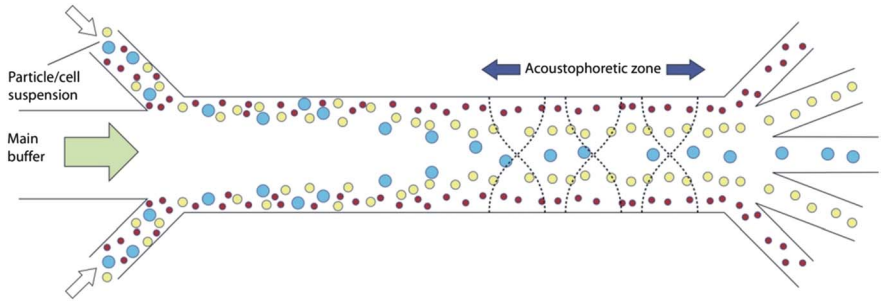

Fig. 6 Schematic of free flow acoustophoresis for multiplex separation of mixed suspensions.

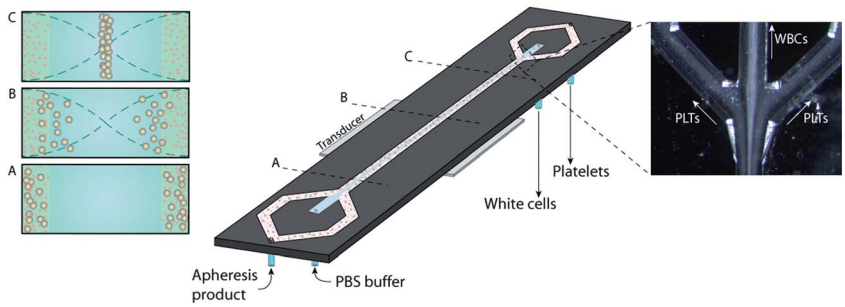

Fig. 7 Schematic of system setup for platelet removal in apheresis product. Figures to the left are cross-section schematics of the cell locations in the acoustic standing wave in the channel. (A) The sample enters from the side outlets in the channel. (B) and (C) The larger cells (peripheral blood progenitor cells and leukocytes) experience a higher force than the smaller cells (platelets) and are thus transferred earlier to the centre of the channel. By balancing the flow and acoustic power, the leukocytes can be separated from the platelets. The right side inset shows a still image of an ongoing dual outlet FFA of apheresis product from patients undergoing hematopoietic stem cell treatment. PBPCs are seen focused into the central outlet together with the leukocytes (light grey band) and the platelets are flowing into the side outlets (grey bands).

magnetic forces are employed.[39] Combinations of acoustics with other forces will be covered more in detail in the forthcoming Acoustofluidics tutorial no. 23. SAW based separation of cells has also been reported where platelets and red blood cells were separated based on their different acoustophoretic mobilities.[40]

A fundamental mode of FFA is to extract two fractions of a mixed population, one *via* the central outlet with larger particles and a smaller sized population *via* the side outlet. Hence, in recent years the use of FFA to divide a sample population into two different cohorts based on their acoustophoretic mobilities has been investigated and reported in several microfluidic applications. Thevoz *et al.*[14] showed that FFA can be used to distinguish between cells in different phases of the cell cycle where the breast cancer cell line MDA-MB-231 was investigated and cells in G2/M and S phases (larger size) moved faster in the acoustic force field towards the channel centre and were removed *via* the central outlet, leaving a purified fraction of G1 cells (smaller size) in the side outlets.

The rising interest in concentrating circulating tumor cells by means of microfluidic approaches has also spurred efforts in the acoustophoresis field. Augustsson *et al.*[41] described a dual outlet FFA system for the enrichment of tumor cells (TCs) spiked into blood samples. Red blood cells were lysed and the remaining white blood cell (WBC) population with the TCs were subjected to FFA, providing an enriched TC fraction in the central outlet. The WBC discrimination could be tuned by the system flow rate. At a TC recovery of about 50% (flow rate 800 microlitre per minute) all WBCs were directed to the side outlet.

Dykes *et al.* recently reported on an analogous dual FFA system for the removal of excess platelets in peripheral blood progenitor cell (PBPC) apheresis products. The system relied on the higher acoustophoretic mobility of PBPCs relative platelets and hence a purified fraction of PBPCs was obtained in the central outlet, Fig. 7. A mean recovery of WBC of 98% and a depletion of 89% of the platelets were achieved in a set of ten patient samples. It was also shown that platelet activation was low and that the viability of the PBPC was unchanged after undergoing acoustophoresis.[42]

The strategy of using FFA to separate a suspension in two size distributions lends itself very well also to a serial connection of these devices to enable extraction of a population of a narrow size distribution. Adams and Soh[43] demonstrated a "band-pass" particle size filtering, efficiently discriminating 3, 5 and 10 micrometre polystyrene particles by this principle, Fig. 8. This approach to particle sizing is similar to the multiple outlet FFA described by Petersson *et al.*[38] with the beneficial difference that the size cut-off for the low pass and high pass bands can be tuned independently of each other. On the other hand two piezodriver systems are required. In the case of the multiple outlet FFA the size cut-off is defined by the flow rate at each outlet relative to the total flow rate.

Size separation by frequency switching. An alternative mode of separation, which like FFA also is based on the magnitude of the primary acoustic radiation force, is the use of frequency switching such that the acoustic resonator is switched between different resonance modes at controlled time intervals. If the amplitude for the employed actuation frequencies and the actuation intervals are tuned accordingly, an alignment of two particle categories into the different pressure nodes of the two frequencies respectively can be obtained. This was first explored by Mandralis and Feke in a system that combined an oscillating flow that was synchronized with the frequency switching between a single node and a triple node resonance, so-called synchronized ultrasonic flow field fractionation.[44] If the oscillating flow was defined to have a net flow in one direction the system was able to drive particles larger than a defined size to one end of the flow system and smaller particles to the other end, enabling a continuous mode of operation. An approach resembling this was reported by Siversson *et al.* in a chip

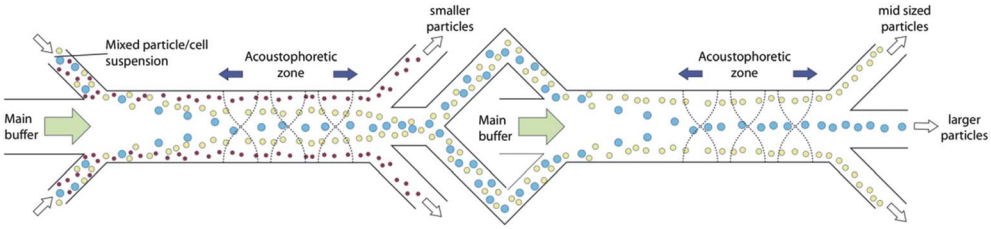

Fig. 8 Schematic of the serially linked dual FFA system as described by Adams, where a "low pass", "band pass" and a "high pass" sizing of microparticles were reported.[43]

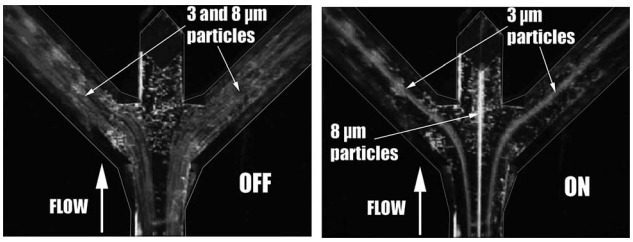

Fig. 9 Left, mixed particle suspension (3 and 8 micrometre beads) streaming through the acoustophoresis channel without ultrasound active. Right, ultrasonic frequency switching between fundamental $\lambda/2$ resonance at 2 MHz and the $2\lambda/2$ resonance at 4 MHz. Reproduced by permission from The Royal Society of Chemistry.[1]

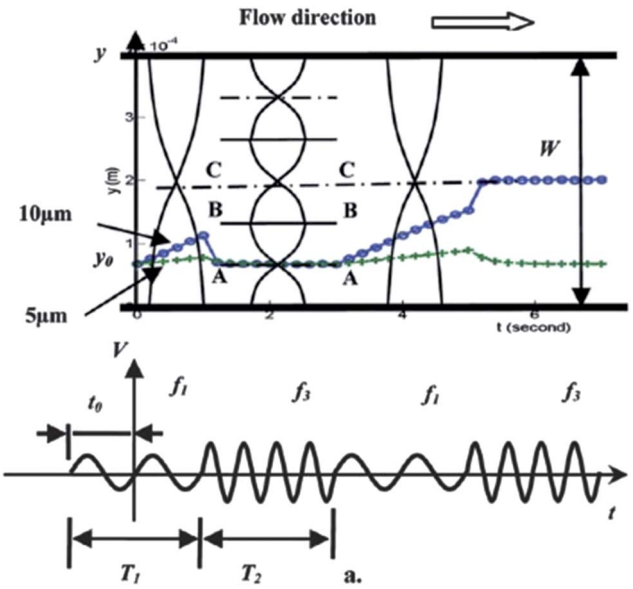

Fig. 10 Schematic of particle separation by frequency switching as outlined by Liu and Lim.[46] The top figure shows the two operational modes with the fundamental resonance, f_1, initially applied during the period T_1, which is indicated in the amplitude *vs.* time diagram below. During time period T_2 the frequency is tripled, f_3, generating three nodes that align the cells along the node closest to the sidewall indicated by A. As the frequency again is switched to f_1, larger particles (blue) move faster against node C, passing the position indicated by B. As the frequency again is switched to f_3 smaller beads (green) are retrieved into the A node whereas larger particles (blue) progress towards the central line C. Reproduced by permission from The Royal Society of Chemistry.

integrated solution of ultrasonic resonance mode switching, where 8 micrometre polystyrene particles were separated in a continuous flow from 3 micrometre particles, Fig. 9.[45]

More recently Liu and Lim described a similar approach where controlled switching between $3\lambda/2$ and $\lambda/2$ resonances (5.6 and 1.8 MHz) enabled separation of 10 and 5 micrometre polystyrene beads.[46] Fig. 10 illustrates nicely the trajectories of the beads as they undergo a repetitive frequency switching.

A general observation when performing separation by frequency switching is that it requires a solid process control if results are to be generated over an extended period of time. Fine tuning of duty cycles and actuation amplitudes is critical. It is also recommended that a temperature control of the chip be implemented. It should be pointed out that temperature control is a general requirement for long-term stable operation, as primarily the speed of sound and hence resonance are dependent on temperature. Recently Augustsson *et al.* demonstrated the importance of a strict temperature control while performing acoustophoresis experiments.[47] The beauty of separation by frequency switching is that it offers a continuous flow based mode of operation, where the separation parameters are solely dependent on the electronic driving of the piezo ceramic actuator.

Separation by binary acoustophoresis. Binary acoustophoresis utilizes the fact that in a given buffer two particle types may display significantly different acoustic contrast factors. In the case where the contrast factor for a particle type has an opposite sign (different polarity) relative to its counterpart, the primary acoustic radiation force acts in the opposite direction. Particles in aqueous systems, with a density higher than water and a positive acoustic contrast factor, will experience a radiation force towards the standing wave pressure node, whereas particles of lower density and a negative contrast factor will focus onto the pressure antinodes. Gupta *et al.* demonstrated binary acoustophoresis in an early paper, where polyethylene particles of two different densities suspended in 30% glycerol

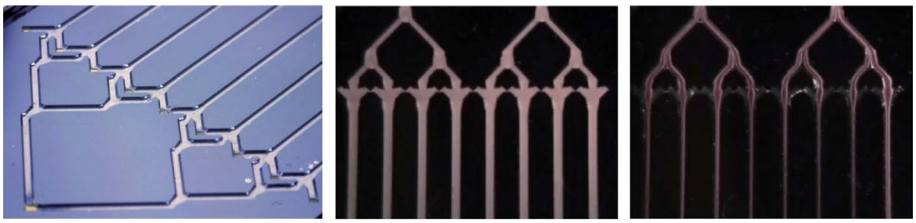

Fig. 11 Increasing throughput in continuous flow acoustophoresis. Left, close-up of the outlet zone of the silicon microfabricated eight parallel channel acoustophoresis chip. Middle, blood streaming through the channel without applying ultrasound. Right, simultaneous actuation of all channels and focusing of blood in the centre of each channel and collection *via* an outlet bifurcation network.

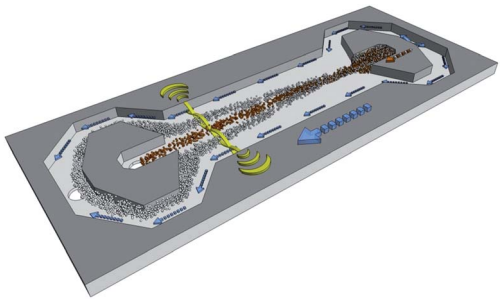

Fig. 12 Schematic of multi-node actuation for the separation of lipid particles in milk, such that lipids are directed to the side outlets and the remaining micelles and milk fluid can be accessed for FTIR analysis *via* the centre outlet. Courtesy of Carl Grenvall.

displayed opposite polarities in the acoustic contrast factor.[48]

The first chip integrated binary acoustophoresis separation was reported by Peterson *et al.* where erythrocytes and lipid particles were separated in a microsystem, extracting erythrocytes free from lipid microemboli in blood recovered from major surgery.[49,50] As a means to increase sample throughput parallel channel configurations can be realized, yet actuated by a single transducer. Along this line Jönsson *et al.*[51] demonstrated continuous blood processing for lipid emboli removal at 500 microlitre per minute in an eight parallel channel configuration, Fig. 11. Systems based on planar resonator configurations hold a potential to high throughput performance as the separation channels in those setups are extended in a plane and actuation is performed orthogonal to the plane. Ebbesen *et al.* reported a 17 mm wide planar resonator that performed separation of particles and cells in the range of 1 L h^{-1}.[9] More detailed discussion on planar resonators will be given in the Acoustofluidics tutorial 9 in this series.

Binary separation has also been utilized in applications of foodstuff quality control where a system for raw milk sample pretreatment prior to Fourier transform infrared spectroscopy (FTIR) analysis was proposed by Grenvall *et al.*[52] The acoustophoresis setup depleted the lipid emulsion from the milk by focusing these in the pressure antinode (white particles, Fig. 12) of an acoustic standing wave, providing a clarified milk fluid with casein micelles (indicated as the brownish particles in Fig. 12). The removal of the lipid emulsion from the milk enabled direct FTIR analysis of the protein and lactose content in the clarified fraction. Also, improved conditions for lipid analysis was obtained in the enriched lipid fraction. The binary separation was performed in a multi-node configuration where the milk sample was laminated in the centre of the acoustophoresis channel. As the system was actuated in a $3\lambda/2$-resonance mode lipids were forced to the nearest antinode off centre. Thereby lipid aggregation along the channel sidewalls and hence disturbed laminar flow properties were avoided, allowing continuous operation over an extended period of time, Fig. 12.

In situations where particles or cells display equal acoustophoretic mobility and cannot be adequately separated by acoustophoresis, there may still be an option to tune the experiment such that for example a binary separation can be performed. By formulating a buffer such that the two particles to be separated display opposing polarities, a binary separation should be feasible. Gupta and Feke[48] demonstrated this in 1995 and Petersson *et al.*[38] reported a corresponding microchip based acoustophoresis experiment where two types of particles (polystyrene and PMMA) of 3 micrometre size would not separate in a conventional FFA setup. By tuning the buffer density with caesium chloride (0.22 mg mL^{-1}), a balancing criterion with opposing polarity of the contrast factor was accomplished where 96% of the PMMA particles were collected in the central outlet and 88% of the polystyrene particles were routed to the side outlets.[38]

Measuring acoustophysical properties of cells by means of acoustophoresis

To be able to tune the buffer conditions such that different polarities of the acoustic contrast factor are obtained, knowledge about acoustophysical properties of the species to be separated is required. In the case of cell separation, acoustophysical data of different cell species are not widely available. Acoustophoresis has, however, recently been developed to provide means to measure the compressibility and density of cells in their native state. A basic requirement for this is that the acoustic energy density can be determined in the acoustophoresis channel. Barnkob *et al.* have reported two methods for the estimation of the acoustic

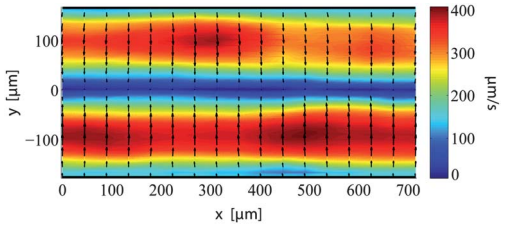

Fig. 13 Acoustophoretic velocity field as derived by PIV measurements during an acoustophoretic focusing event in a half wavelength resonator.[53]

energy density either based on a particle tracking method or by performing particle imaging velocimetry (PIV) using calibration beads of known acoustophysical properties.[47] Fig. 13 shows the particle velocity field in an acoustophoresis channel (1000 micrometre long field of view) as recorded by PIV, which serves as the basis for the calculation of the acoustic energy density. Once the acoustic field is known, particles or cells with unknown properties can be introduced into the channel and the acoustophoretic translation to the central node is again performed. The acoustic contrast factor can be estimated by measuring the time resolved trajectory of the particle/cell and the size.[53] A further development of this method for acoustophysical cell/particle characterization was presented by Barnkob, by using the generalized equation for the primary acoustic radiation force in an arbitrary acoustic field and performing two reference acoustic focusing PIV experiments with different calibration beads, the pressure and velocity gradient fields can be calculated (eqn (3)). For a detailed description of the derivation of the primary acoustic radiation force see Acoustofluidics tutorial 7 in this series.[10] Once these are derived the time resolved tracking of an unknown cell species is performed in the acoustic field and the radius is measured, thereafter both the cell density and the compressibility can be calculated.[54] Hartono *et al.*[55] also recently demonstrated an analogous technique to measure cell properties. The calibration beads were introduced into the acoustophoresis channel simultaneously with the unknown cells and cell and particle trajectories were tracked during the acoustic focusing. The resulting calculations yielded the compressibility of the cells under the assumption of beforehand given cell densities. These developments are truly interesting applications of acoustophoresis, where now rapid and relatively simple experimental procedures can for example provide important biomechanical data of cells in response to different pharmaceutical treatment of cells undergoing different biological states.

Medium switching–cell/bead washing

Since microfluidic channels operate in the laminar flow domain, it is possible to laminate flow streams side by side in a channel. By applying a standing wave field across the flow channel it is possible to move particles from one buffer stream to another and thus complete the medium/buffer switch. This step equals a centrifugal wash step where the sample is centrifuged, decanted and the pellet re-suspended in new buffer. Hawkes *et al.* reported a layered separator in glass and silicon which comprised two inlets and two outlets that generated two parallel streams.[12] A sample containing yeast cells and fluorescein was introduced in the lower stream and the cells were consequently elevated into the clean flow stream when the ultrasound was turned on, Fig. 14A. This resulted in about 90% of the fluorescein being washed from the yeast cells.

Petersson *et al.* used a similar setup in a transversal separator but utilized a system with three parallel streams in an axisymmetrical configuration where the two outer streams were the sample streams.[56] The input sample was composed of polyamide beads mixed with Evans blue as a traceable contaminant compound. The half wavelength standing wave moved the particles from the sample streams into the clean buffer present in the centre of the channel, Fig. 14B. Wash efficiency was monitored by absorbance measurement at the Evans blue absorbance peak in the two fractions. Wash

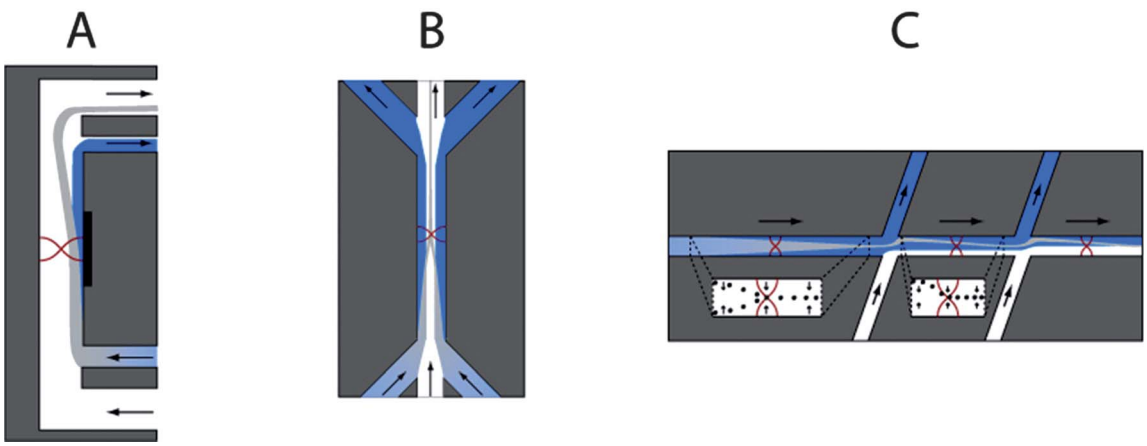

Fig. 14 Different principles of medium switching. (A) The layered resonator by Hawkes *et al.*[12] where particles are elevated into the clean buffer. (B) The transversal resonator by Petersson *et al.*,[56] where particles are translated from the sample streams along the sides into the pressure node in the clean buffer. (C) The side-washer by Augustsson *et al.*[59] where the original buffer is gradually removed by sideways shifting of the carrier buffer while the sample stays focused in the channel centre by the standing wave forces.

efficiencies (contaminant removal) of about 95% were reported at bead concentrations of 1.5% volume fraction. For increased wash efficiency, sequential steps can be realized on the same silicon wafer.[57] It should also be noted that the wash efficiency decreases with increasing bead concentration. Therefore a given situation for performing bead/cell washing will have to be adapted to its specific conditions.

The same design was also used by Lenshof *et al.* where unbound fluorescent label was washed from the sample prior to FACS analysis.[58] Labeled cells in suspension entered from the side inlets and were transferred into the clean centre buffer while the unbound label remained in the original suspension. This wash step is usually done manually by sequential centrifugation steps. Acoustophoresis eliminates the need for centrifugation steps and the analysis time can thus be decreased, reducing the risk of sample-handling errors.

A slightly different approach was suggested by Augustsson *et al.* where wash fluid was infused *via* multiple inlets along one side of the main flow and buffer was withdrawn at equal rates along corresponding outlets along the opposing channel wall.[59] The chip consisted of a main channel with eight side branches on each side of the main channel. The side branches introduced wash buffer on one side of the chip and removed the corresponding fraction of the original buffer on the opposing side. The cells and microbeads were retained in the centre of the channel by the primary acoustic radiation force while the surrounding buffer was sequentially shifted sideways. The original buffer was completely replaced after five side washing steps, Fig. 14C only shows two of the eight side branches. The grey central trace indicates the trajectory of the cells/particles along the buffer exchange channel.

Translating particles across laminar interfaces allows rapid on-line change of buffers. This has been capitalized in systems where rare species, be that molecular or microbial, are targeted in a complex matrix. By introducing microbeads with an affinity specific ligand that binds selectively to the target species, the bead can work as the pull-out engine for the rare species from the complex matrix into a clean buffer. This is accomplished by assuring that the beads have relatively high acoustophoretic mobility as compared to the undesired components that compose the complex matrix. Microfluidic acoustophoresis based affinity bead extraction systems have been described by Augustsson *et al.*[60] A more thorough description of affinity acoustophoresis will be covered in the forthcoming Acoustofluidics tutorial no. 11.

Acoustic valving and switching

The possibility to shift particles into other streamlines, as outlined in Fig. 14A, enables the principle of valveless switching of particles and cells. By constructing a bifurcation tree of channels, which are actuated by different transducers, it is possible to direct particles to given outlets. A device with two inlets and four different addressable outlets was demonstrated by Laurell *et al.*[1] The two transducers were driven at different frequencies to avoid crosstalk between the excitation regions. By actuating the transducers at a certain scheme as depicted in Fig. 15, the switching of particles or particle streams to a designated outlet was demonstrated, following a binary sequence of activating the transducers.

The cross-talk problem between neighboring resonances was investigated by Manneberg *et al.* where the resonance spreading effect was both simulated and measured by PIV in a system for continuous flow particle switching and merging.[61] It was concluded that channels of different widths could be used with transducers designed for that specific channel width without severe resonance cross-talk in other regions of the chip. They also designed a 'split-chip' in which particle tracks could be selectively combined as an acoustic field was applied over the active region, see Fig. 16. This is the opposite version of the binary sorting described previously and could be used to merge particles into controlled populations.

Acoustic FACS strategies

The step from valving and switching of particles to fluorescence activated cell sorting (FACS) utilizing acoustic standing wave forces is not very far. The conventional FACS instrumentation uses an external force, usually an electric field, to divert cells in droplets to a pre-designated collection bin. The modal change from an electrostatic force on droplets to acoustically activated forces on targeted cells in a continuous flow truly poses some engineering challenges. The standard way of operating an acoustically driven rare event sorter is to introduce particles in a stream laminated along one sidewall. As a rare event is detected, *e.g.* by fluorescence, the ultrasonic standing wave is actuated and the particle will be moved to the pressure node and hence translated into a different flow stream having a separate outlet, thus completing the sorting. This principle of sorting was used by Johansson *et al.* and, as illustrated in Fig. 17, the cells pass the interrogation zone A and if sorted they end up in region B, otherwise in zone C.[63] The acoustic FACS demonstrated a sorting rate of 3 particles per second.

In order to increase the sorting rate of an acoustic FACS, it is important that the sample arrives at the sorting point at the same position every time. If the sample enters the sorting region at an arbitrary position in the parabolic flow profile the time of arrival to the acoustic switching zone will vary considerably and thus define a maximum throughput which is low in relation to a theoretical maximum if all cells travelled at the same speed through the system. Grenvall *et al.* solved this problem by introducing a pre-focusing region operated at a higher frequency which would not cross-talk with the sorting frequency.[64] The pre-focusing standing wave comprised three pressure nodes and the particles were pre-focused in the node closest to the sidewall. At the same time a vertical half wavelength resonance was obtained, locating the particles into a confined zone in the cross-section of the channel next to the sidewall, giving the particles a uniform flow velocity. The reduced velocity distribution increased the switching frequency and the prototype system reported a switching frequency of 50 Hz.

Manneberg *et al.* demonstrated in a similar manner that 2-dimensional confinement of particles in the cross-section of a flow channel can reduce velocity distributions of the particles. In this case they used two transducers, one

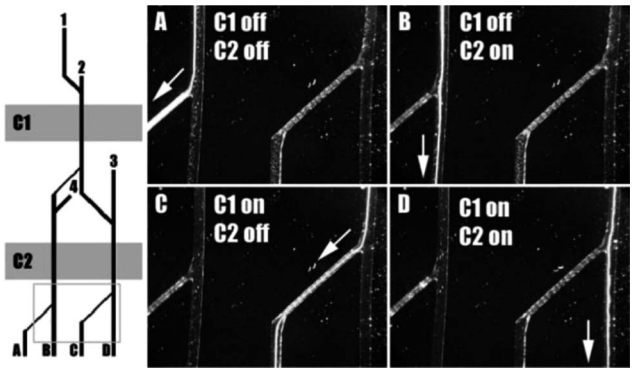

Fig. 15 Acoustic valving of particles by sequential activation of two transducers in a binary sequence enabled addressing of particles to four outlets by the acoustic control setting. From Sundin *et al.*[62] Reproduced by permission from The Royal Society of Chemistry.[1]

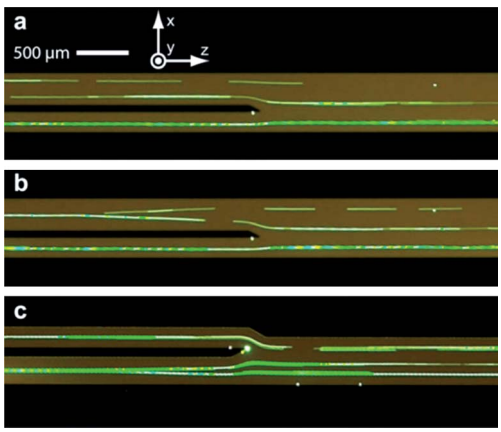

Fig. 16 Demonstration of addressable merging of particle tracks by Manneberg *et al.*[61] Note that the flow direction in the image is from right to left. Reprinted from Manneberg *et al.*[61] Copyright (2009), with permission from Elsevier.

for lateral focusing and one for the vertical mode.[65]

Franke *et al.* used a slightly different approach as they used a SAW device which utilized acoustic streaming to induce a movement of the sample fluid.[66] The device was realized in a PDMS structure with three inlets and two outlets on a substrate with an interdigitated transducer (IDT), which generated the surface acoustic waves, see Fig. 18. The sample was hydrodynamically focused and if no ultrasound was applied the sample followed the left stream out. When the IDT was turned on, acoustic streaming bent the sample jet and caused the bead to divert into the right outlet and complete the sorting. The SAW FACS showed sorting numbers of 2000 cells per second and a viability test was performed on the sorted cells concluding that no harm was done to the cells.

Combining acoustophoresis with other orthogonal force fields

The literature reports a series of papers on combinations of acoustic techniques with other force fields such as magnetophoresis,[39] dielectrophoresis[24] and electrostatic forces.[17,67] These multiplex approaches will not be discussed herein and the reader is referred to the oncoming issue in this tutorial series, Acoustofluidics tutorial no. 23.

Working with cells in acoustophoretic systems

When changing target species from particles to viable cells in acoustic separation systems, a new set of aspects needs to be considered. Viable cell handling is challenging due to the stringent environmental conditions for cell survival on account of the fragile nature of the cell membrane.[68,69] The maintenance of optimal cell conditions is vital to preserve the expected lifetime of the cells. If viable cells are not needed for subsequent analysis, cell membrane stabilization (fixation) will facilitate the cell handling. Fixation can be performed with cross-linking reagents such as paraformaldehyde (PFA) or with organic solvents such as methanol. Cell fixation terminates any ongoing biochemical reaction and stabilizes the cells.[70] For fixed cells the amount of time spent on cell processing is generally of little relevance. However, for viable cells the time needed for subsequent biochemical steps, *e.g.* fluorescent staining, washing, *etc.*, should be minimized. Cell mortality generally increases with longer handling times. Depending on cell type, the cells should be handled on ice, at room temperature or at 37 °C. The optimal handling temperature will reduce cell damage and death for sensitive cell populations.

FACS analysis can be used to identify and quantify the separated cell populations.[41] For non-fixed cells it is advisable to analyse the outlet fractions immediately. Fixed cells can be stored in the fridge and analysed the following day.

For optimal acoustic separation, fresh cell samples are preferable. The cell samples should thus be prepared directly before the acoustic separation. For example, blood samples stored overnight have a tendency to contain more aggregated cells, which aggravate the acoustic cell separation.

Acoustophoresis is a gentle separation method, and generates no immediate or long-term changes in cell viability or cell proliferation[41,42] when operated under typical acoustophoretic separation conditions with energy densities in the range of 10–100 J m^{-3}. It should be noted that temperature control is recommended not only to maintain a fixed resonance in the chip but also that chip heating may induce cell damage if the piezo is operated at higher voltages. There will be more details on cell viability and biocompatibility in Acoustofluidics tutorial 12.

Particle size limitations in acoustophoresis

When performing acoustophoresis experiments, commonly particle/cell size ranges from single micrometres to 10–20

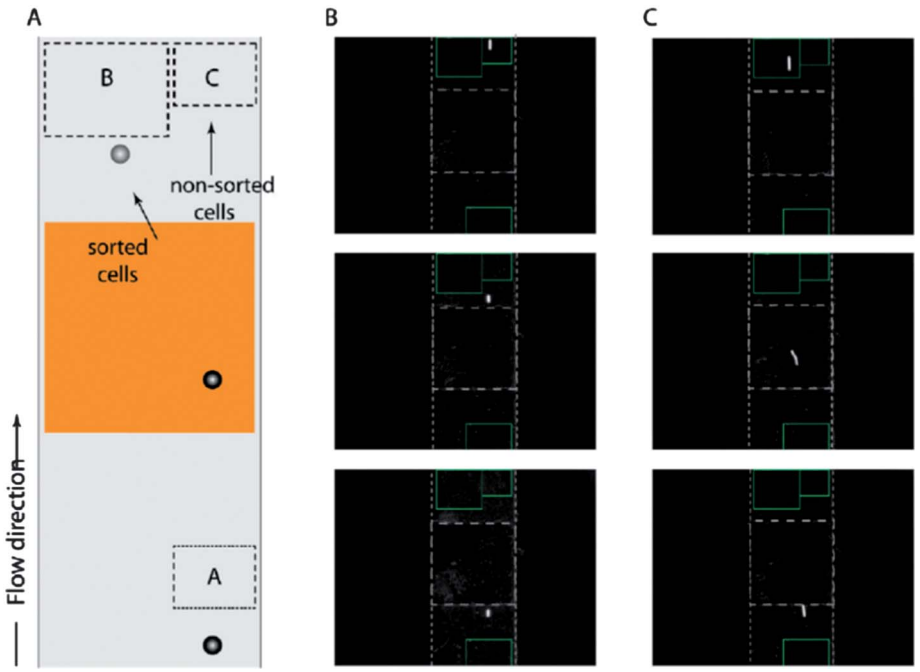

Fig. 17 Schematic of the cell sorter by Johansson *et al.*[63] (A) The excitation of the transducer (orange rectangle) is controlled by the optical fluorescent detection of a cell in detection zone A. Sorted cells end up in zone B and non-sorted in zone C. (B) Image where a particle is not actively sorted. (C) The white particle is deflected using an acoustic standing wave and is directed to zone B. Reprinted with permission from Johansson *et al.*[63] Copyright (2009) American Chemical Society.

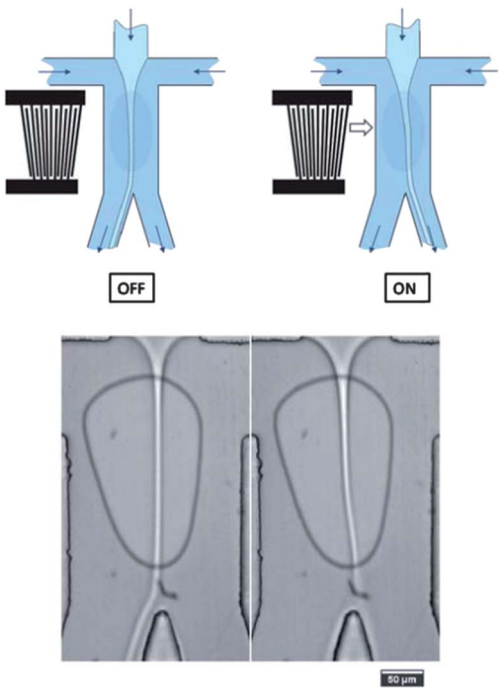

Fig. 18 The main channel is hydrodynamically focused by flow through the two side channels. Without applying a surface acoustic wave the jet of the main channel moves into the left outlet channel due to its lower hydrodynamic resistance (OFF, left). When switching on the SAW, acoustic streaming is induced and deflects the focusing stream into the right channel outlet (ON, right). From Franke *et al.*[66] Reproduced by permission from The Royal Society of Chemistry.

micrometres. The lower size limit where the primary acoustic radiation force is effective is about 1 micrometre. This is based on the fact that the mobility of a particle driven by the primary acoustic radiation force scales with the square of the radius and at a particle size around 1–2 micrometres (depending on density and compressibility) hydrodynamic forces generated by acoustic streaming equal the effective primary acoustic radiation force at an actuation frequency of 2 MHz.[71] Means to move beyond this limit can be accomplished by reducing the dimensions of the acoustic resonator, hence increasing the actuation frequency. The primary acoustic radiation force scales proportional with the operating frequency. By driving the acoustic system with a frequency that scans across the optimal resonance a suppression of streaming artifacts can be accomplished. Ohlin *et al.* demonstrated that acoustic streaming in microwells can be reduced by scanning the actuation frequency (2.13 MHz) over a 200 kHz bandwidth.[72] The upper size limit is commonly set by the fact that sedimentation becomes a considerable problem. If compensation of the buffer composition in terms of the buoyancy of the particle is performed, an

extended working range can be accomplished.

Quantifying separation performance

The quantification of particle or cell separations performed by acoustophoresis is a continuous challenge and many times the development of protocols to validate the performance of the executed separations is an effort equal to the development of the actual experimental setup. When working with microparticles in the micrometre size range, Coulter counting is many times a straightforward method. It should, however, be commented that the lower limit of detection in conventional Coulter counting is in the range of 1 micrometre, and the noise level at lower sizes rises dramatically. Coulter counting provides absolute particle counts and yields excellent size distribution data. It should be mentioned that the most commonly expressed disadvantage of Coulter counting is the frequent tendency to clog the measuring orifice and hence mainly analytically pure systems without the tendency for particle aggregation should be employed. When working with cell based systems fluorescence activated cell sorting, FACS, is an evident technique to use when characterizing the content of a sample with mixed cell populations. However, cell specific labeling protocols prior to FACS analysis are often required. The obtained data are composed of measurements of forward- and side-scattered light as well as fluorescence intensity and the software included with the instruments commonly allows elaborate data mining. As an alternative to the above flow based techniques, cell/particle counting can be performed manually by traditional counting in a Bürcher chamber. This offers operator control and visual inspection of the sample composition, which sometimes may provide information that is not revealed in FACS or Coulter counting. The drawback is evidently the tedious manual work when extended studies are performed. A simple but rather crude method to quantify particle concentrations in different outlet fractions of an acoustophoresis experiment is to use standard sedimentation capillaries that are centrifuged and the height of the solid matter in the sample is derived as a measure of the particle concentration. It is a simple and fast method but does not reveal any information about size distribution or different species in the sample and the accuracy of the measurement is quite rough.

Conclusions

Acoustophoresis integrated in microfluidics systems has developed rapidly in the past few years and matured to a level where new applications now are appearing at an increasing rate. Specifically, it can be seen that opportunities in developing new modalities for advanced cell handling in microenvironments are emerging where the combination of controlled fluidic conditions with a spatial control of cells or particles provides novel tools within cell biology and biomedical applications.

This tutorial tries to cover the most recent developments of applications within the acoustophoresis field. An emphasis is put on continuous flow based systems operated in the transversal mode, as other acoustophoresis modalities will be covered in subsequent tutorial of this series.

Acknowledgements

Financial support is acknowledged from Swedish Research Council (VR 621-2010–4389), Vinnova Innovationer för Framtidens Hälsa—CellCARE, Formas –TvärLivs—Dnr: 222-2010-413.

References

1 T. Laurell, F. Petersson and A. Nilsson, *Chem. Soc. Rev.*, 2007, **36**, 492–506.
2 A. Lenshof and T. Laurell, *Chem. Soc. Rev.*, 2010, **39**, 1203–1217.
3 J. D. Adams, U. Kim and H. T. Soh, *Proc. Natl. Acad. Sci. U. S. A.*, 2008, **105**, 18165–18170.
4 N. Gadish and J. Voldman, *Anal. Chem.*, 2006, **78**, 7870–7876.
5 M. P. MacDonald, G. C. Spalding and K. Dholakia, *Nature*, 2003, **426**, 421–424.
6 M. Yamada, M. Nakashima and M. Seki, *Anal. Chem.*, 2004, **76**, 5465–5471.
7 L. R. Huang, E. C. Cox, R. H. Austin and J. C. Sturm, *Science*, 2004, **304**, 987–990.
8 J. A. Davis, D. W. Inglis, K. J. Morton, D. A. Lawrence, L. R. Huang, S. Y. Chou, J. C. Sturm and R. H. Austin, *Proc. Natl. Acad. Sci. U. S. A.*, 2006, **103**, 14779–14784.
9 C. L. Ebbesen, J. D. Adams, R. Barnkob, H. T. Soh and H. Bruus, in *Micro Total Analysis Systems 2010*, Groningen, Netherlands, 2010, pp. 728–730.
10 H. Bruus, *Lab Chip*, 2012, **12**, 1014.
11 N. R. Harris, M. Hill, S. Beeby, Y. Shen, N. M. White, J. J. Hawkes and W. T. Coakley, *Sens. Actuators, B*, 2003, **95**, 425–434.
12 J. J. Hawkes, R. W. Barber, D. R. Emerson and W. T. Coakley, *Lab Chip*, 2004, **4**, 446–452.
13 A. Nilsson, F. Petersson, H. Jonsson and T. Laurell, *Lab Chip*, 2004, **4**, 131–135.
14 P. Thevoz, J. D. Adams, H. Shea, H. Bruus and H. T. Soh, *Anal. Chem.*, 2010, **82**, 3094–3098.
15 J. J. Shi, X. L. Mao, D. Ahmed, A. Colletti and T. J. Huang, *Lab Chip*, 2008, **8**, 221–223.
16 J. J. Shi, H. Huang, Z. Stratton, Y. P. Huang and T. J. Huang, *Lab Chip*, 2009, **9**, 3354–3359.
17 K. Yasuda, S. S. Haupt, S. Umemura, T. Yagi, M. Nishida and Y. Shibata, *J. Acoust. Soc. Am.*, 1997, **102**, 642–645.
18 K. Yasuda, S. Umemura and K. Takeda, *Jpn. J. Appl. Phys.*, 1995, **34**, 2715–2720.
19 G. Goddard and G. Kaduchak, *J. Acoust. Soc. Am.*, 2005, **117**, 3440–3447.
20 G. Goddard, J. C. Martin, S. W. Graves and G. Kaduchak, *Cytometry, Part A*, 2006, **69**, 66–74.
21 A. Lenshof, M. Evander, T. Laurell and J. Nilsson, *Lab Chip*, 2012, **12**, 684–695.
22 N. R. Harris, M. Hill, R. Townsend, N. M. White and S. P. Beeby, *Sens. Actuators, B*, 2005, **111**, 481–486.
23 M. Evander, A. Lenshof, T. Laurell and J. Nilsson, *Anal. Chem.*, 2008, **80**, 5178–5185.
24 M. Wiklund, C. Gunther, R. Lemor, M. Jager, G. Fuhr and H. M. Hertz, *Lab Chip*, 2006, **6**, 1537–1544.
25 J. J. Hawkes and W. T. Coakley, *Sens. Actuators, B*, 2001, **75**, 213–222.
26 S. Kapishnikov, V. Kantsler and V. Steinberg, *J. Stat. Mech.: Theory Exp.*, 2006, P01012.
27 A. Lenshof, A. Ahmad-Tajudin, K. Jaras, A. M. Sward-Nilsson, L. Aberg, G. Marko-Varga, J. Malm, H. Lilja and T. Laurell, *Anal. Chem.*, 2009, **81**, 6030–6037.
28 P. W. S. Pui, F. Trampler, S. A. Sonderhoff, M. Groeschl, D. G. Kilburn and J. M. Piret, *Biotechnol. Prog.*, 1995, **11**, 146–152.
29 M. Groschl, W. Burger, B. Handl, O. Doblhoff-Dier, T. Gaida and C. Schmatz, *Acustica*, 1998, **84**, 815–822.
30 M. Wiklund, J. Toivonen, M. Tirri, P. Hanninen and H. M. Hertz, *J. Appl. Phys.*, 2004, **96**, 1242–1248.
31 W. T. Coakley, D. Bazou, J. Morgan, G. A. Foster, C. W. Archer, K. Powell, K. A. J. Borthwick, C. Twomey and J. Bishop, *Colloids Surf., B*, 2004, **34**, 221–230.
32 T. Lilliehorn, U. Simu, M. Nilsson, M. Almqvist, T. Stepinski, T. Laurell, J. Nilsson and S. Johansson, *Ultrasonics*, 2005, **43**, 293–303.
33 B. Vanherberghen, O. Manneberg, A. Christakou, T. Frisk, M. Ohlin, H. M. Hertz, B. Onfelt and M. Wiklund, *Lab Chip*, 2010, **10**, 2727–2732.

34 B. Hammarström, M. Evander, H. Barbeau, M. Bruzelius, J. Larsson, T. Laurell and J. Nillsson, *Lab Chip*, 2010, **10**, 2251–2257.
35 J. C. Giddings, *Sep. Sci. Technol.*, 1985, **20**, 749–768.
36 D. A. Johnson and D. L. Feke, *Sep. Technol.*, 1995, **5**, 251–258.
37 M. Kumar, D. L. Feke and J. M. Belovich, *Biotechnol. Bioeng.*, 2005, **89**, 129–137.
38 F. Petersson, L. Aberg, A. M. Sward-Nilsson and T. Laurell, *Anal. Chem.*, 2007, **79**, 5117–5123.
39 J. D. Adams, P. Thevoz, H. Bruus and H. T. Soh, *Appl. Phys. Lett.*, 2009, **95**, 254103.
40 J. Nam, Y. Lee and S. Shin, *Microfluid. Nanofluid.*, 2011, **11**, 317–326.
41 P. Augustsson, C. Magnusson, C. Grenvall, H. Lilja and T. Laurell, in *Micro Total Analysis Systems 2010*, Groningen, Netherlands, 2010, pp. 1592–1594.
42 J. Dykes, A. Lenshof, I. Åstrand-Grundström, T. Laurell and S. Scheding, *PLoS One*, 2011, **6**, e23074.
43 J. D. Adams and H. T. Soh, *Appl. Phys. Lett.*, 2010, **97**, 064103.
44 Z. I. Mandralis and D. L. Feke, *AIChE J.*, 1993, **39**, 197–206.
45 C. Siversson, F. Petersson, A. Nilsson and T. Laurell, in *Micro Total Analysis Systems 2004*, 2005, vol. 2, pp. 330–332.
46 Y. Liu and K. M. Lim, *Lab Chip*, 2011, **11**, 3167–3173.
47 P. Augustsson, R. Barnkob, S. T. Wereley, H. Bruus and T. Laurell, *Lab Chip*, 2011, **11**, 4152–4164.
48 S. Gupta, D. L. Feke and I. Manas-Zloczower, *Chem. Eng. Sci.*, 1995, **50**, 3275–3284.
49 F. Petersson, A. Nilsson, C. Holm, H. Jonsson and T. Laurell, *Analyst*, 2004, **129**, 938–943.
50 F. Petersson, A. Nilsson, C. Holm, H. Jonsson and T. Laurell, *Lab Chip*, 2005, **5**, 20–22.
51 H. Jönsson, C. Holm, A. Nilsson, F. Petersson, P. Johnsson and T. Laurell, *Ann. Thorac. Surg.*, 2004, **78**, 1572–1578.
52 C. Grenvall, P. Augustsson, J. R. Folkenberg and T. Laurell, *Anal. Chem.*, 2009, **81**, 6195–6200.
53 P. Augustsson, R. Barnkob, C. Grenvall, T. Deierborg, P. Brundin, H. Bruus and T. Laurell, in *Micro Total Analysis Systems 2010*, Groningen, Netherlands, 2010, pp. 1337–1339.
54 R. Barnkob, P. Augustsson, C. Magnusson, H. Lilja, T. Laurell and H. Bruus, in *Micro Total Analysis Systems 2011*, Seattle, Washington, USA, 2011, pp. 127–129.
55 D. Hartono, Y. Liu, P. L. Tan, X. Y. S. Then, L. L. Yung and K. M. Lim, *Lab Chip*, 2011, **11**, 4072–4080.
56 F. Petersson, A. Nilsson, H. Jonsson and T. Laurell, *Anal. Chem.*, 2005, **77**, 1216–1221.
57 P. Augustsson, J. Persson, S. Ekstrom, M. Ohlin and T. Laurell, *Lab Chip*, 2009, **9**, 810–818.
58 A. Lenshof, B. Warner and T. Laurell, in *Micro Total Analysis Systems 2010*, Groningen, Netherlands, 2010, pp. 1577–1579.
59 P. Augustsson, L. B. Aberg, A. M. K. Sward-Nilsson and T. Laurell, *Microchim. Acta*, 2009, **164**, 269–277.
60 J. Persson, P. Augustsson, T. Laurell and M. Ohlin, *FEBS J.*, 2008, **275**, 5657–5666.
61 O. Manneberg, S. M. Hagsater, J. Svennebring, H. M. Hertz, J. P. Kutter, H. Bruus and M. Wiklund, *Ultrasonics*, 2009, **49**, 112–119.
62 M. Sundin, A. Nilsson, F. Petersson and T. Laurell, in *Micro Total Analysis Systems 2004*, 2005, vol. 1, pp. 662–664.
63 L. Johansson, F. Nikolajeff, S. Johansson and S. Thorslund, *Anal. Chem.*, 2009, **81**, 5188–5196.
64 C. Grenvall, M. Carlsson, P. Augustsson, F. Petersson and T. Laurell, in *Micro Total Analysis Systems 2007*, ed. J.-L. Viovy, P. Tabeling, S. Descroix and L. Malaquin, Paris, France, 2007, pp. 1813–1815.
65 O. Manneberg, J. Svennebring, H. M. Hertz and M. Wiklund, *J. Micromech. Microeng.*, 2008, **18**, 095025.
66 T. Franke, S. Braunmuller, L. Schmid, A. Wixforth and D. A. Weitz, *Lab Chip*, 2010, **10**, 789–794.
67 K. Yasuda, K. Takeda and S. I. Umemura, *Jpn. J. Appl. Phys.*, 1996, **35**, 3295–3299.
68 S. J. Singer and G. L. Nicolson, *Science*, 1972, **175**, 720.
69 K. Simons and D. Toomre, *Nat. Rev. Mol. Cell Biol.*, 2000, **1**, 31–39.
70 L. C. Javois, *Methods in Molecular Biology, Vol. 115. Immunocytochemical Methods and Protocols*, Humana Press Inc., Totowa, NJ.
71 R. Barnkob, P. Augustsson, T. Laurell and H. Bruus, in *Micro Total Analysis Systems 2010*, Groningen, Netherlands, 2010, pp. 1247–1249.
72 M. Ohlin, A. E. Christakou, T. Frisk, B. Onfelt and M. Wiklund, in *Micro Total Analysis Systems 2011*, Seattle, Washington, USA, 2011, pp. 1612–1614.